Lotus Shaped Negative Curvature Hollow Core Fiber with 10.5 dB/km at 1550 nm Wavelength

M. B. S. Nawazuddin, *Member, IEEE*, N.V. Wheeler, J.R. Hayes, *Member, OSA,* S.R. Sandoghchi, *Member, IEEE*, *Member, OSA,* T.D. Bradley, *Member, OSA*, G. Jasion, *Member, IEEE*, R. Slavík, *Senior Member, IEEE, Fellow, OSA*, D.J. Richardson, *Fellow, IEEE, Fellow, OSA* and F. Poletti, *Member, IEEE*

***Abstract*— We present a novel Lotus shaped negative curvature antiresonant hollow core fiber with the potential for low loss and very wide bandwidth. A minimum loss of ~10 dB/km at 1550 nm and less than 100 dB/km over a bandwidth of ~650 nm is demonstrated, with effectively single mode behaviour over lengths of a few tens of meters. We demonstrate power penalty free 10.5-Gbit/s data transmission through an 85 m length of fiber at both O and C telecom bands. The fiber macro bend sensitivity has also been tested, which is relevant for telecom as well as for other applications including beam delivery and gas based sensing. The bend loss is found to be below 0.2 dB/m for bend radii down to 8 cm at wavelengths away from the short wavelength edge of the transmission band.**

***Index Terms*—Fiber optics communications, hollow core optical fibers, low latency, microstructured optical fibers.**

I. Introduction

Due to the unique guidance mechanisms offered by hollow core photonic crystal fibers (HC-PCFs), which enable light transmission in low index media such as air and vacuum, these fibers are great contenders for applications in low latency data communications [1,2]. Furthermore, they also have potential use in gas based linear/non-linear optics, laser and particle guidance and high power, ultra-short pulse delivery [3,4]. Based on their guidance mechanism, HC-PCFs are broadly categorised as hollow core photonic bandgap fibers (HC-PBGFs) and hollow core antiresonant/inhibited coupling fibers (HC-ARF). Within the broad HC-ARF category, many different fiber topologies have emerged, such as those with a Kagome cladding (K-HCF) [5-7], or a simpler structure with a single ring of touching or non-touching/non-contact tubes as antiresonant elements [8-12].

To date, HC-PBGFs still offer the lowest loss recorded for HC-PCFs, although this comes at the expense of useable bandwidth, only 10s of nm in the lowest loss fiber [13]. While this can be extended to up to ~200 nm, this yields some compromise on the minimum loss [2]. On the other hand, in recent years the loss in K-HCFs, which offer octave wide bandwidth, has improved so much that at certain wavelengths they can already compete with HC-PBGFs, albeit with an increased bend loss [6, 7]. The main reason behind such dramatic recent improvement has been the realization of the importance of imposing a negative curvature hollow core boundary [5, 8 and 10-12].

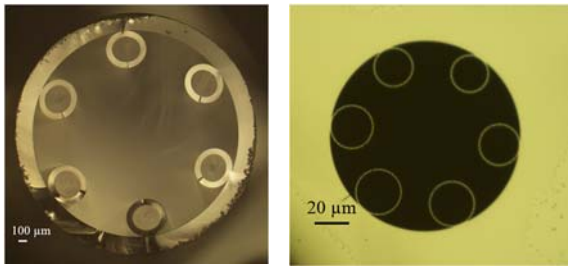

(a) (b)

Fig. 1: (a) Microscope image of a cane, (b) Microscope image of a fabricated typical single ring NCTHC-ARF

Early works observed that a K-HCF with a negative curvature core wall significantly reduced attenuation as compared to the standard core geometry [5]. These fibers were soon followed by attempts to reduce the cladding complexity by using a single ring of non-contacting tubes (NCT) surrounding the core. This was found to allow not only a faster preform preparation compared to HC-PBGFs or K-HCFs, but also in certain cases a lower transmission loss and a wider bandwidth [9, 12]. However, one of the main practical challenges in the fabrication of such non-contact tubular hollow core ARFs (henceforth referred to as NCTHC-ARF) is to achieve the required high structural uniformity in: (i) the gap between the non-contact tubular elements and (ii) the size (and by mass conservation the thickness) of each glass tube. To illustrate the typical non-uniformities that can be observed in these fibers, we show in Fig. 1 an example of a single ring NCTHC-ARF fabricated in our group. While this is only one example, all NCTHC-ARFs reported to date seem to qualitatively present these undesirable features [8, 9 and 11].

The optical microscope image of the cane (or primary

This work is supported by an ERC (grant agreement no. 682724) and by the Royal Society.

All authors are with the Optoelectronics Research Centre, University of Southampton, Southampton, SO17 1BJ, UK (e-mail:m.b.syed-nawazuddin@soton.ac.uk; nvw1v10@orc.soton.ac.uk; jrh@orc.soton.ac.uk; srs1g12@soton.ac.uk; T.Bradley@soton.ac.uk; G.Jasion@soton.ac.uk; r.slavik@soton.ac.uk; djr@orc.soton.ac.uk; frap@orc.soton.ac.uk).

preform) is shown in Fig. 1a. From this image, the cane structure appears symmetric. Yet, fiber fabricated from this cane (Fig. 1b) has non-uniform gaps between the tubular elements; this prevents narrow gaps between the elements being achieved without some of the tubes contacting each other. Pressurisation during the fiber draw accentuates any small initial differences between the tubes that may be present in the cane. In this case, this introduces 10-20% differences in the size of all the tubular elements. The increased gap between the tubes increases the leakage loss in such fibers, while any difference in the wall thicknesses of the single ring tubular elements will contribute to wider resonance peaks, which narrow the transmission bandwidth.

Here, we address these fabrication limitations by including additional smaller diameter capillaries in between the original tubes to help maintain a uniform gap between the antiresonant elements. This type of NCTHC-ARF is regarded as having a "Lotus" shaped core which is formed during the fiber drawing by the equilibrium between gas pressure in the holes and the surface tension of the fiber material. We have published some preliminary results of this work in [14].

II. Fiber Design and Fabrication

The schematic drawing of the primary stack design is shown in Fig. 2. We chose 6 uniform capillaries with a diameter of ~3.9 mm to make the preform which eventually form the main antiresonant tubular elements and a further 6 additional capillaries (smaller by a factor of 2) are included between the larger capillaries and the jacket tube. The core capillary shown in the center is used only at either end of the initial preform to support the stacked capillaries prior to drawing.

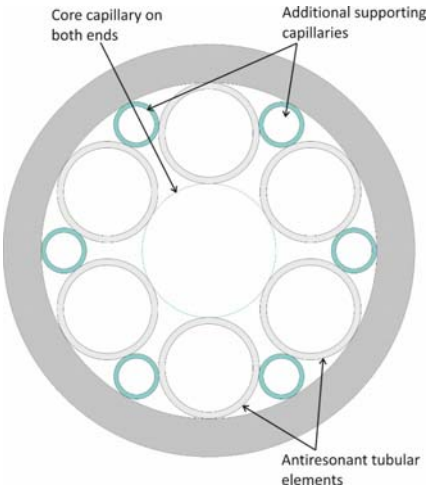

Fig. 2: Schematic drawing showing the cross section of the stack design

To fabricate the Lotus shape NCTHC-ARF, we used the standard two stage stack and draw technique. The cross section of fabricated cane and fiber are shown in Fig. 3a and 3b respectively. As can be seen, a small and very uniform gap between the large tubes is achieved in both the cane (Fig. 3a) and the fiber (Fig. 3b). This is essential to minimise leakage loss through the gaps [15]. The critical fiber parameters such as the core radius, core wall thickness, microstructure radius and the fiber outer diameter are controlled by modifying the draw parameters. The structural dimensions of the fabricated fiber are shown in Fig. 4. The measured structural dimensions show exceptional uniformity in terms of gap between the tubes and radius of the antiresonant tubular elements. It has a core diameter of 40 µm (defined as the maximum diameter of a circle that can be inscribed inside the core), an average antiresonant tube radius of 18.6 µm (with a standard deviation of 0.27 µm) and the average tube thickness is ~425 nm. The mean gap between the tubes is 2.6 µm (with a standard deviation of 0.07 µm). Table I shows a comparison of geometrical parameters of the Lotus NCTHC-ARF with a 7 tube NCTHC-ARF developed in our group [9].

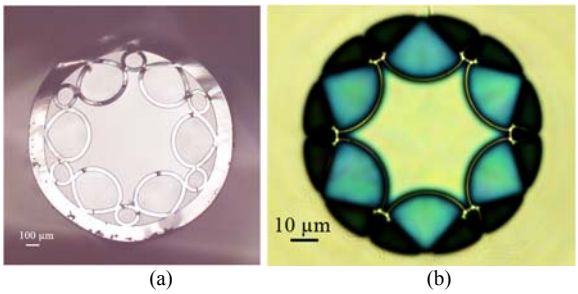

(a) (b)

Fig. 3: Microscope image showing cross sections of the fabricated: (a) cane and (b) Lotus NCTHC-ARF

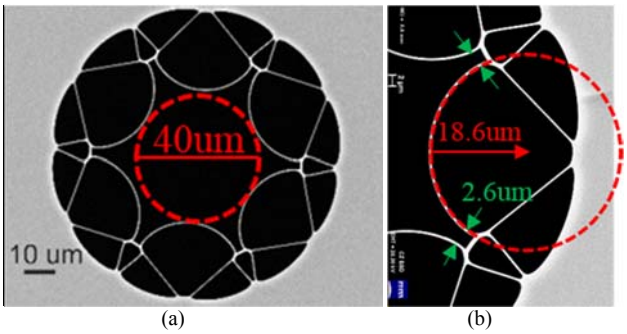

(a) (b)

Fig. 4: Electron micrograph of the full fiber cross section showing (a) core diameter, (b) antiresonant tubular element dimension and inter-tube gap

TABLE I
Comparison of Lotus shaped NCTHC-ARF with 7 Tube NCTHC-ARF

Fiber	Mean cap. radius (µm)	Mean Inter-tube gap (µm)	Core radius (µm)	Membrane thickness (nm)
7 tube NCTHC-ARF [9]	22.9±0.84	5.4±1.1	20	359
Lotus shape NCTHC-ARF	18.6±0.27	2.6±0.07	20	425

While the additional small spacing tubes are very effective in

increasing the cross-sectional uniformity of the structure, they also lead to the presence of nodes, where the big and small capillaries contact. These nodes can act as independent waveguides, introducing additional resonances in the spectrum. However, the negative curvature in the core surround wall helps to introduce a radial separation between the core modes and the high loss glass modes guided in the nodes, which significantly reduces coupling between them.

III. Fiber Characterisation and Modelling

A. Attenuation

To measure the loss of the Lotus shape NCTHC-ARF, a cutback loss measurement was carried out on a 111m long sample. The fiber was loosely coiled on the measurement bench to a diameter of ~30 cm. A white light source was launched into the fiber through a butt-coupled launch fiber with a closely matched mode field diameter. An optical spectrum analyser (OSA, 400-1750 nm) was used to measure the transmission spectrum. The measured transmission and loss spectra are shown in Fig. 5. The lowest loss measured is 9.8 dB/km at 1612 nm and a loss of 10.5 dB/km is observed at 1550 nm. This presents the lowest loss recorded at a wavelength of 1550 nm with a NCTHC-ARF to date. The fiber shows a wide operational bandwidth, with loss <100 dB/km over significantly more than ~650 nm, measured with a conventional optical spectrum analyser. The measured bandwidth is not inherently limited by the fiber design but rather by the spectral response of the OSA on the long wavelength edge. Around 1245 nm and 1332 nm, two loss peaks of ~50/70 dB/km are noticeable, which we interpret as resonance peaks caused by the nodes where the big and small tubular elements contact. However, these do not prevent the fiber operating in the C and L telecoms bands.

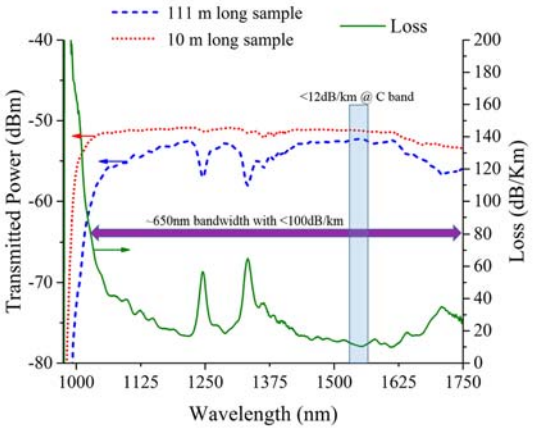

Fig. 5: Measured transmission spectra of 111 m (blue-dash) and 10 m (red-dots) cut back length with the calculated cut back loss (green)

B. Modelling

A theoretical study was performed to identify the effect and contribution of these struts/nodes. To identify the main structural features responsible for the low loss in the fiber, two additional geometries were modelled using Comsol. The 2D cross section of the fiber was modelled in Comsol to find the mode fields and confinement losses. The surface scattering loss is also estimated from the normalized electric field at the interfaces. The methods we followed to do these simulations are similar to those explained in detail in Ref. [15]. The structural diagrams of all three geometries along with their simulated mode field patterns are shown in Fig. 6. In all three structures, the core radius and curvature of the antiresonant elements remain the same. Fig. 6(a) shows the fabricated NCTHC-ARF having the full lattice lotus structure. The arc only geometry shown in Fig. 6(b) has core surround arcs with the same curvature as the fabricated fiber, which continue all the way to the jacket, however, it does not have the smaller tubes and the nodes associated. In the extended arc geometry (see Fig. 6(c)), the outer jacket is pushed further away to allow the arcs to continue into an almost tubular structure.

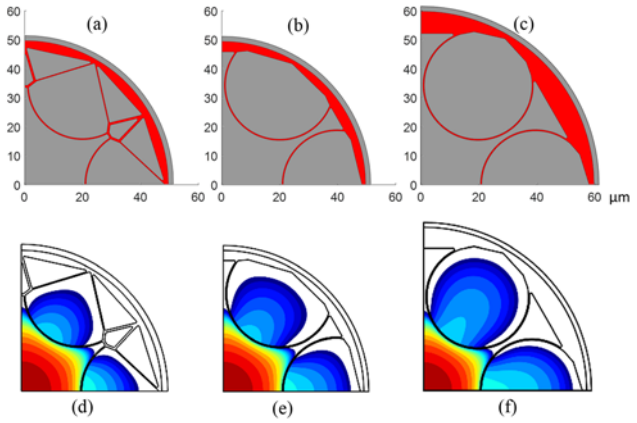

Fig. 6: Structural schematics of three different geometries: (a) full lattice lotus structure, (b) arc only geometry and (c) extended arc geometry and their corresponding simulated mode field patterns: (d), (e) and (f).

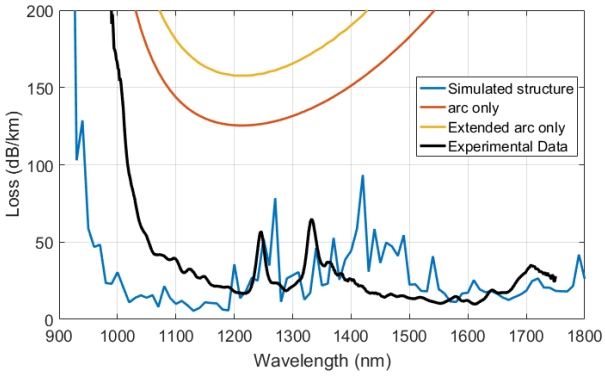

Fig. 7: Calculated loss (including both confinement and scattering contributions) of all three geometries compared with the measured cutback loss of the Lotus shaped NCTHC-ARF

Fig. 7 shows the calculated loss (including both confinement and scattering contributions) of all three geometries, compared with the experimentally measured loss. As can be seen, the simulated loss of the full lattice lotus structure lies in a similar range to the measured loss, and the presence of some loss peaks

(although not exactly at the same spectral position) is also captured by the simulations. In contrast, the calculated loss of the other two geometries having no nodes is over one order of magnitude higher. The reason for such higher loss in both nodeless geometries (Fig. 6b and c) is that the air modes guided in the capillaries are close in effective index to the fundamental core mode, as they have very similar sizes, and thus they can easily phase match (see simulated mode field patterns shown in Fig. 6e and f). However in the complete lattice lotus structure the tube area is decreased by the presence of the straight elements at the back of the tubes, and these struts act as reflectors preventing the mode field from extending as far into the solid cladding (see Fig. 6(d)). The simulations also indicate that the observed total attenuation in this fiber is dominated by confinement loss (CL). One way to reduce the dominating CL in the HC-AR fibers is to have a large core diameter. However, the large core increases the bend loss significantly. The Lotus fiber presented here has core diameter of ~40 µm, which is chosen as an optimum value to have low CL and bend loss.

The novel Lotus shaped NCTHC-ARF presented here clearly shows that the additional tubes are very effective in allowing the realisation of a uniform gap distribution and size of the tubular elements. As a consequence of this, the loss can be significantly reduced, from ~30 dB/km at telecom wavelengths in Ref. [9] to only ~10 dB/km in this work. Note that if one wanted to use a nodeless structure (both geometries 2 and 3 in Fig. 6b and 6c), the use of 7 or 8 tubes has been found to provide better results [8, 9, and 12].

C. Bend Loss

To understand the bend robustness in this fiber and also to explore the possibility of using this fiber for beam delivery applications, macro bend loss measurements were carried out. For this experiment, before including a bend, the transmission for the effectively straight condition is measured with an OSA. Without disturbing the input coupling and the output port, the fiber is bent on a board having different bend radii ranging from 20 cm down to 8 cm.

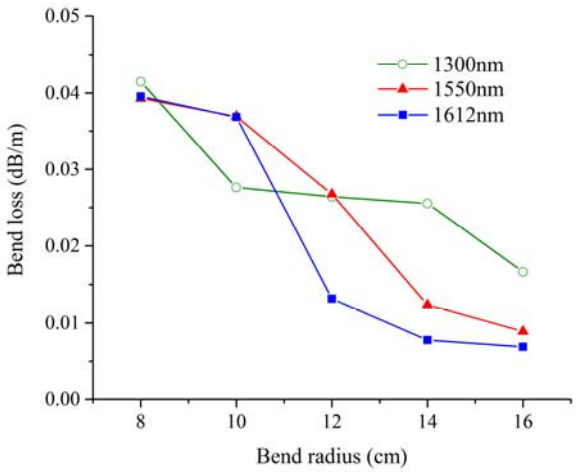

Fig. 8: Measured bend loss as a function of bend radius

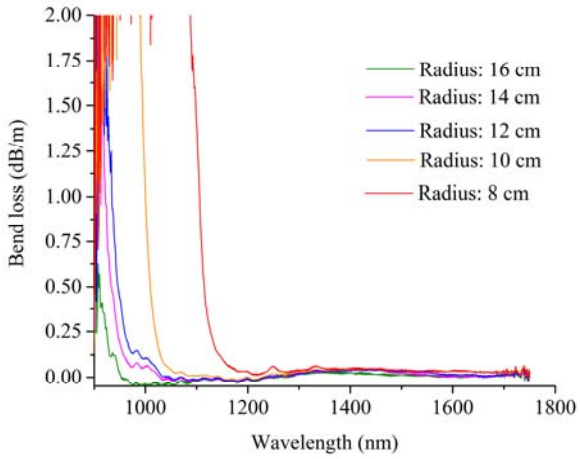

Fig. 9: Bend loss as a function of wavelength for different bend radii

The length of the fiber used for this measurement is ~12 m. The bend loss as a function of radius for three different wavelengths is shown in Figure 8. Down to bend radii of 8cm, the attenuation due to bends for all three wavelengths does not change significantly.

The wavelength 1300 nm lies in between the two high loss resonances due to the nodes/struts, however the bend loss is not increased by their presence, as compared to wavelengths further away. Besides, the resonance peaks due to the two struts/nodes are not affected by the bend. However, we notice a considerable shift of the short wavelength edge with decreasing bend radii, as shown in Fig. 9. From this and from the results in Fig. 8 one can see that at a coiled diameter of ~30 cm our cutback loss measurements at 1612 nm and 1550 nm in Fig. 5 have negligible contribution from bend loss.

D. S^2 measurement

As in any conventional large core fiber, HC-ARFs support higher order modes (HOMs) [16, 17]. It is known, however, that a mode stripping mechanism exists that significantly attenuates most HOMs [15] in some HC-ARF designs.

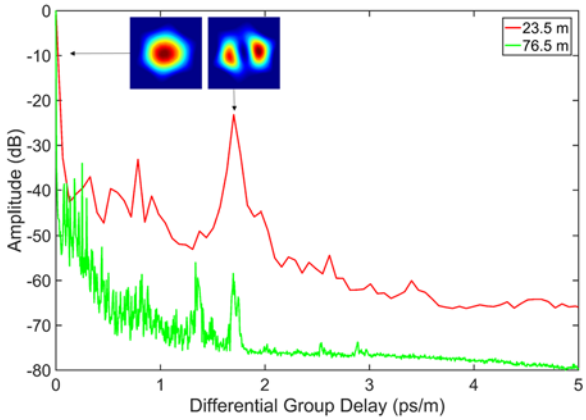

Fig. 10: Group delay curve showing the mode content of the fiber at two different lengths: 23.5m and 76.5m

To quantify the degree of HOM existence in this fiber, S^2 measurement was performed on two different lengths of fiber.

The measured results for short (23.5m) and long (76.5m) length samples at 1550 nm are shown in Fig. 10. The inset shows the reconstructed mode field intensity distribution of the fundamental mode and of the higher order LP_{11} mode for a short length fiber of ~23.5m. As can be seen, there is some residual LP_{11} mode after 23.5m, however it becomes practically non-existent (down to about 60 dB) after 76.5m, indicating that on long enough lengths (a few tens of metres) the fiber is essentially single mode.

IV. Data Transmission Experiment

A 10.5-Gbit/s on-off keyed data transmission experiment was performed on the fiber to assess its potential in communications applications. We selected two wavelengths to demonstrate transmission in the two primary telecomm bands: at 1310 nm (O band) and 1550 nm (C band). The 1310 nm wavelength lies in between the two additional resonances introduced by the nodes/struts around the core, and it allows us to check whether these introduce any performance degradation. While 1550 nm is centred in the lowest loss region. To test the fiber under more challenging circumstances and study the effect that splices might have, we spliced a 10m tail of the same fiber to the 76.5m previously tested with S^2, using a conventional arc-fusion splicer. Due to the short lengths (and low total attenuation) involved, we were able to use a single mode fiber (SMF28) with a mode field diameter of ~10 μm butt-coupled to both input and output side of the test fiber, despite the fairly large coupling loss that this caused (~14.5dB) due to the large mode field diameter mismatch. At 1550 nm we also used a fiber pigtailed isolator to avoid any back reflection of light into the transmitter. At the receiver side the signal was analyzed with a bit error ratio (BER) tester.

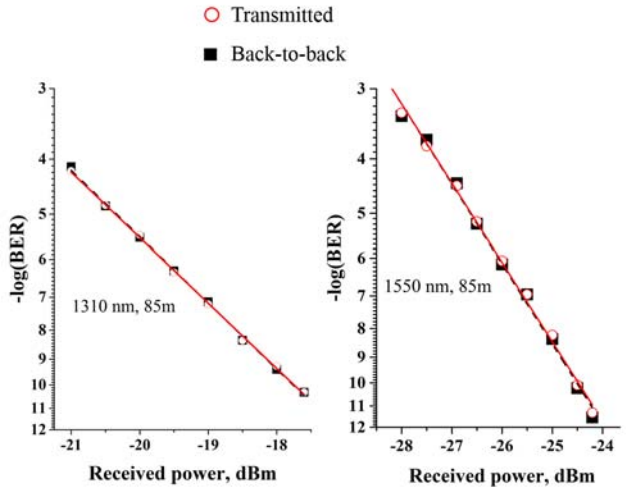

(a) (b)

Fig. 11: BER of two different transmission wavelengths in (a) 1310nm (O band) and (b) 1550nm (C band). Also shown are the back-to-back measurements without any fiber.

Despite the additional cladding resonances near 1300 nm, the presence of a splice of the NCTHC-ARF to itself and the use of severely sub-optimal launch and collection fibers, error free (BER< 10^{-10}) data transmission was achieved through the full 86m length at both wavelengths. Fig. 11 shows the resulting BER, compared with back-to-back measurements. In both instances, the BER curves show no power penalty, which is to be expected given the excellent modal properties of the fiber after such a propagation distance.

V. Conclusions

We have demonstrated a novel negative curvature hollow core antiresonant fiber with a Lotus shaped core. With additional small capillaries in the cladding structure, an exceptional structural uniformity in terms of the size of each antiresonant tubular element and the inter-tube distance is achieved. This regularity was key to produce the lowest transmission loss reported so far at 1550 nm for hollow core fibers guiding by antiresonance, of around 10 dB/km. The fiber exhibits a very wide bandwidth of well over 650 nm with <100 dB/km attenuation. The drawback of the presence of cladding nodes where the small stabilization tubes touch the antiresonant ones is that two resonance peaks appear in the spectrum. However, their position can be kept outside the telecoms C and L bands, and their influence on data transmission was shown to be negligible. The good modal purity and effectively single mode behavior of the fiber after a few tens of meters, measured through S^2 measurement, was exploited to transmit data. We demonstrated penalty free 10.5-Gbit/s transmission through an 86m length of fiber (containing one splice to itself) in two different telecom bands: O and C. Bend loss measurements show low loss for bends down to 8cm in diameter at wavelengths away from the short wavelength edge. With further loss reduction by introducing additional nested tubes within the lotus structure [15], these fibers could become serious contenders for applications such as low latency data transmission applications, for transmission of light below the silica Rayleigh scattering limit in the spectral range UV-VIS-NIR, high energy pulse laser beam delivery and gas based non-linear optics.

Acknowledgment

This work is supported by an ERC (grant agreement no. 682724) and by the Royal Society.

All data supporting this study are openly available from the University of Southampton repository at http://doi.org/10.5258/SOTON/D0335

References

[1] F. Poletti, N. V. Wheeler, M. N. Petrovich, N. Baddela, E. N. Fokoua, J. R. Hayes, D. R. Gray, and D. J. Richardson, "Towards high-capacity fiber-optic communications at the speed of light in vacuum," *Nature Photonics*, vol. 7, no. 4. pp. 279–284, 2013.

[2] Y. Chen, Z. Liu, S. R. Sandoghchi, G. T. Jasion, T. D. Bradley, E. N. Fokoua, J. R. Hayes, N. V Wheeler, D. R. Gray, B. J. Mangan, R. Slavík, F. Poletti, M. N. Petrovich, and D. J. Richardson, "Multi - kilometer Long, Longitudinally Uniform Hollow Core Photonic Bandgap Fibers for Broadband Low Latency Data Transmission," *J. Light. Technol.*, vol. 34, no. 1, pp. 104–113, 2016.

[3] F. Benabid and P. S. J. Russell, "Hollow core photonic crystal fibers: a new regime for nonlinear optics and laser-induced guidance," *Proc. of 6th International Conference on Transparent Optical Networks*, vol.2, pp. 84-90, 2004.

[4] C. Saraceno, F. Emaury, A. Diebold, I. Graumann, M. Golling and U. Keller, "Trends in high-power ultrafast lasers", *Proceedings of SPIE*, vol. 9835, pp. 98350X-1, 2016.

[5] Y. Y. Wang, N. V. Wheeler, F. Couny, P. J. Roberts, and F. Benabid, "Low loss broadband transmission hypocloid-core Kagome hollow core photonic crystal fiber", *Optics Letters*, 36(5), 669-671, 2011.

[6] N.V. Wheeler, T.D. Bradley, J.R. Hayes, M.A. Gouveia, Y. Chen, S.R. Sandoghchi, F. Poletti, M.N. Petrovich and D.J. Richardson, "Low loss kagome fiber in the 1 um wavelength region", *Specialty Optical Fibers Meeting at the Advanced Photonics Congress*, Canada, SoM3F.2, 1pp, 2016.

[7] N. V. Wheeler, T. D. Bradley, J. R. Hayes, M. A. Gouveia, S. Liang, Y. Chen, S. R. Sandoghchi, S. M. Abokhamis Mousavi, F. Poletti, M. N. Petrovich and D. J. Richardson "Low loss Kagome hollow core fibers operating from the near- to the mid-IR", *Optics Letters,* vol. 42, No.13, pp. 2571-2574, 2017.

[8] A. D. Pryamikov, A. S. Biriukov, A. F. Kosolapov, V. G. Plotnichenko, S. L. Semjonov, and E. M. Dianov, "Demonstration of a waveguide regime for a silica hollow core microstructured optical fiber with a negative curvature of the core boundary in the spectral region > 3.5 μm," *Optics Express* 19(2), 1441 – 1448, 2011.

[9] J. R. Hayes, S. R. Sandoghchi, T. D. Bradley, Z. Liu, R. Slavík, M. A. Gouveia, N. V Wheeler, G. Jasion, Y. Chen, E. N. Fokoua, M. N. Petrovich, D. J. Richardson, and F. Poletti, "Antiresonant Hollow Core Fiber With an Octave Spanning Bandwidth for Short Haul Data Communications", *J. Lightwave Technol.*, vol. 35, no. 3, p. 437, 2017.

[10] F. Yu and J. C. Knight, "Negative Curvature Hollow Core Optical Fiber", *IEEE Journal of selected topics in Quantum Electronics*, vol. 22, no. 2, 4400610, pp1-10, 2016.

[11] Wei, C., R. Joseph Weiblen, C. R. Menyuk and J. Hu (2017). "Negative curvature fibers: publisher's note." Advances in Optics and Photonics 9(3): 562-562

[12] B. Debord, A. Amsanpally, M. Chafer, A. Baz, M. Maurel, J. M. Blondy, E. Hugonnot, F. Scol, L. Vincetti, F. Gerome and F. Benabid, "Ultra low transmission loss in inhibited-coupling guiding hollow core fibers", *Optica*, vol. 4, no. 2, pp. 209-217, 2017.

[13] B. J. Mangan, L. Farr, A. Langford, P. J. Roberts, D. P. Williams, F. Couny, M. Lawman, M. Mason, S. Coupland, R Flea and H. Sabert, "Low loss (1.7 dB/km) hollow core photonic bandgap fiber", *PDP Optical Fiber Communication Conference*, PDP24, 8230423, pp1-3, 2004.

[14] M. B. S. Nawazuddin, N. V. Wheeler, J. R. Hayes, T. Bradley, S. R. Sandoghchi , M. A. Gouveia, G. T. Jasion, D. J. Richardson and F. Poletti, "Lotus shaped negative curvature hollow core Fiber with 10.5 dB/km at 1550 nm Wavelength", *in Proc. of 43rd ECOC,* Paper Tu.1.A.2, 2017.

[15] F. Poletti, "Nested antiresonant nodeless hollow core fiber," *Opt. Express*, vol. 22, pp. 23807–23828, 2014.

[16] T. D. Bradley, N. V. Wheeler, G. T. Jasion, , D. Gray, J. R. Hayes, M. A. Gouveia, S. R. Sandoghchi, Y. Chen, F. Poletti, D. J. Richardson, and M. Petrovich, "Modal content in hypocycloid Kagomé hollow core photonic crystal fibers" *Optics Express*, pp. 15798-15812, 24 (14) 2016.

[17] V. Bock, M. Plötner, O. De Vries, J. Nold, N. Haarlammert, T. Schreiber, R. Eberhardt, and A. Tünnermann, "Modal content measurements (S^2) of negative curvature hollow-core photonic crystal fibers", *Optics Express,* 25 (4), pp. 3006-3012, 2017.